Article

The Highly Selective Discovery of Allosteric Ligands from Herbal Extracts through Their Direct Interactions with the Immobilized Headless CaSR Truncation

XianGang Shi, Ru Xu, MeiZhi Jiao, YaoKun Han, ShouCheng Zhao, YiLong Chen, YiYing Xu, FengWu Li, and ChaoNi Xiao*

Read Online

ACCESS | Metrics & More | Article Recommendations

ABSTRACT: Allosteric modulators represent a novel paradigm to therapeutically target G-protein-coupled receptors (GPCRs), but the discovery of novel allosteric ligands from natural products remains challenging. Here, we developed a high-performance affinity chromatography method for screening allosteric ligands toward the human calcium-sensing receptor (CaSR) by immobilizing an extracellular domain-deleted CaSR truncation (ΔCaSR) onto silica gels as solid-phase materials for column packing. The immobilized ΔCaSR column demonstrated the greatest allosteric responsive feature when cinacalcet at 0.50 μM or NPS2143 at 0.25 μM was included in the mobile phase, suggesting that the binding affinity of Ca^{2+} was increased 8% by cinacalcet and was decreased 77% by NPS2143. The column was applied to screen allosteric ligands from Epimedii Folium, which were identified as epimedin B, epimedin C, and icariin using HPLC-MS. The allosteric binding of the screened compounds was testified through competitive experiments, and their allosteric effects were verified by CaSR downstream signaling events, like the intracellular Ca^{2+} levels and cAMP production. Our observations indicated that the three compounds exerted an allosteric effect similar to that of cinacalcet and might be potential allosteric ligands. The proposed approach features the immobilization of headless GPCR truncations, in which the transmembrane domain is exposed to interact directly with the ligands, realizing the highly selective discovery of allosteric ligands from complex herbal extracts.
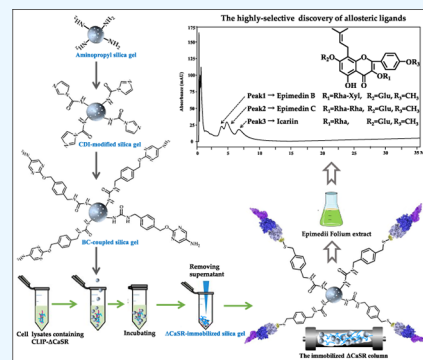
1. INTRODUCTION

G protein-coupled receptors (GPCRs) make up the largest class of cell surface proteins and thus constitute the most important therapeutic drug targets. Allosteric drugs, which interact with binding sites topologically remote from the orthosteric binding pocket, are advantageous over orthosteric drugs with improved selectivity and safety, representing a novel paradigm to therapeutically target GPCRs.[1] However, only 18 allosteric drugs have earned approval from the U.S. Food and Drug Administration (Allosteric Database), partly due to the slow discovery process of new allosteric ligands using conventional methods.[2] Therefore, there is an urgent need for a breakthrough in the development of screening methods.

At present, the application of conventional methods in discovering allosteric ligands faces huge challenges. Cell-based functional screening assays, which measure GPCR downstream signaling effectors, are the current standard; however, they are at risk of missing active allosteric ligands due to inadequate assay conditions and even opposite activities for the same allosteric ligand with the use of different probes.[3] Radioligand binding assays assess receptor–ligand interactions on cell surfaces, which in part reflects the inability to devise a binding assay for low-affinity ligands and is increasingly restricted due

to high production costs and hazards to human health. Other technological approaches, such as fluorescence resonance energy transfer (FRET) and bioluminescence resonance energy transfer (BRET), can circumvent the major limitations of functional assays and radioligand binding assays for discovering allosteric ligands.[4] These technologies normally consist of three steps: the N-terminal domain of the GPCR is truncated and replaced by GFP, then a fluorescent or dyed probe binding the 7-transmembrane domain is identified, and the assay can be screened in the end. Nevertheless, the double labeling of both the probe and receptor requires careful compound design and optimization owing to the impact of fluorophore attachment on ligand affinity and efficacy.[5] Biophysical methods, including affinity selection-mass spectrometry (AS-MS), surface plasmon resonance (SPR), and
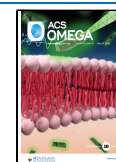
nuclear magnetic resonance (NMR), have been employed in the identification of GPCR ligands;[6,7] however, they require highly purified and stabilized receptors, which are not feasible for a number of target proteins. It is most difficult to determine if a ligand is acting allosterically with GPCRs, since an allosteric ligand introduces texture into pharmacological responses, which need to modify the affinity or the signal imparted to the receptor by the concomitant binding of an orthosteric ligand. An ongoing challenge in the field is how to differentiate allosteric ligands directly from orthosteric ligands.

Among GPCRs, the human calcium-sensing receptor (CaSR) is especially amenable to allosteric modulation owing to its highly modular architecture. It is composed of a large extracellular amino-terminal domain (ECD), a seven-transmembrane domain (7TMD) comprising seven α-helices with interconnecting intracellular and extracellular loops, and a large intracellular carboxy-terminal domain (ICD). The endogenous and exogenous orthosteric ligands, such as Ca^{2+}, di- and trivalent cations (Mg^{2+}, Gd^{3+}), spermine, and polyamines, mainly reside within the ECD, whereas synthetic allosteric ligands (cinacalcet, NPS-R568, calindol, NPS2143, and calhex 231) are located predominantly within the 7TMD.[8−10] CaSR signaling is initiated by Ca^{2+}, which triggers an intermolecular conformational change leading to rearrangement of the 7TMD that, in turn, enables G protein coupling to the intracellular receptor domain. The binding of an allosteric ligand to CaSR engenders a distinct subset of receptor conformations that cannot be achieved through occupancy with an orthosteric ligand alone, thereby altering the orthosteric ligand affinity and the activity of the receptor's active site as well. It was convinced that N-terminally truncated (headless) CaSR resulted in only allosteric ligands interacting within the 7TMD, which are expected to be more selective for targeting the receptor.[11−13] Such a unique structural feature inspired us to develop a new method for the highly selective discovery of allosteric ligands.

The CaSR emerged as the primary mechanism for sensing the extracellular Ca^{2+} stimulus to regulate parathyroid hormone secretion, and it became a good target for a new class of drugs for treating certain bone and mineral disorders. The therapeutic potential of CaSR has been pursued through the development of positive and negative allosteric ligands (PAMs and NAMs, respectively) acting through the 7TMD. Epimedii Folium (Chinese name: YinYangHuo) is a traditional medicinal herb that has long been used to prevent and treat osteoporosis, and the dried leaves of five species have been recorded in the 2020 edition of the Chinese Pharmacopeia. It contains a wealth of chemical components with pronounced pharmacological activities, and more than 200 bioactive compounds have been isolated and identified from it.[14,15] Recent research studies showed that the prenylated flavonoid icariin, the most important representative component of Epimedii Folium, exerted therapeutic effects in vitro involving CaSR.[16,17] Therefore, Epimedii Folium is an attractive natural resource for novel allosteric ligands toward CaSR.

High-performance affinity chromatography with immobilized GPCRs is powerful for separating nonbinders and binders of the target receptor from the complex matrix of an herbal extract. The immobilized β_2-adrenoceptor retained the ability to undergo antagonist- and agonist-induced conformational changes, which can be used to screen for ligands interacting with the resting and active states of the receptor.[18] Inspired by these works, we aimed to establish a chromatographic strategy to screen allosteric ligands targeting CaSR, which includes four key steps: (1) immobilizing the extracellular domain-deleted CaSR truncation (ECD-deleted CaSR, headless CaSR, ΔCaSR) onto microporous silica gels in a one-site manner as solid-phase materials for column packing; (2) evaluating the immobilized ΔCaSR column with regard to ligand-recognition activity and stability; (3) screening allosteric ligands from a herbal medicine; (4) testing the allosteric binding sites of the screened compounds and validating their allosteric effects on the cells.

2. MATERIALS AND METHODS

2.1. Chemicals and Materials. Silica gels (pore size: 300 Å, particle size: 7.0 μm) were acquired from the Lanzhou Institute of Chemical Physics of the Chinese Academy of Sciences. Protein marker, bicinchoninic acid protein assay kit, Fluo-4 AM, and cAMP ELISA kits were purchased from Beyotime Biotechnology Co., Ltd. (Shanghai, China). Yeast extract, peptone, ampicillin, and isopropylthio-β-D-galactoside (IPTG) were achieved from Sigma (St. Louis, MO, USA). Minimum essential alpha medium (α-MEM) was obtained from Wuhan Saiweier Biotechnology Co., Ltd. (Wuhan, China). 2-((4-(Aminomethyl)benzyl)oxy)pyrimidin-4-amine and N,N'-carbonyldiimidazole were bought from Bide Pharmaceutical Technology Co., Ltd. (Shanghai, China). Standards of cinacalcet, NPS2143, epimedin B, epimedin C, and icariin were obtained from Macklin Industrial Corporation (Shanghai, China). Epimedii Folium was bought from Beijing Tongrentang (Xi'an, China).

2.2. Expression of CLIP-Tagged ECD-Deleted CaSR in E. coli Cells. The construct was generated with the fused CLIP tag at the amino terminus of the headless CaSR truncation (abbreviated as ΔCaSR), which is devoid of the 1−612 amino-terminal ECD but includes amino acid residues 613−1078 of full-length human CaSR (ECD-deleted CaSR). The encoded pET15b vector plasmid (customized from Sangon Biotech, Shanghai, China) was transfected into E. coli BL21 (DE3) cells by heat shock. The strains were cultured in LB medium containing ampicillin sodium (100 μg/mL) at 37 °C and 220 rpm. Following 10 h of incubation, a single colony (2−3 mm) was transferred into LB medium (50 mL) and cultivated for 12 h. A small amount of the cells with the expression of ΔCaSR was transferred to LB medium (600 mL) with an 8% inoculation amount for 3 h of incubation at 30 °C, and then IPTG was added at a final concentration of 1.0 mM for an extra 7 h of incubation. A small amount of medium, both before and after induced expression, was collected during culturing for analysis. An ultrasonic cell disruptor (JY92−2, Xinzhi Biotechnology Co., Ltd., Ningbo, China) was used to disrupt the cells buffered in phosphate saline (20 mM, pH 7.4) discontinuously for 40 min. The supernatant of the cell lysates was separated from the precipitate at 12 000 rpm for 15 min at 4 °C in a refrigerated centrifuge (Eppendorf 5804R, Hamburg, Germany).

Sodium dodecyl sulfate-polyacrylamide gel electrophoresis (SDS-PAGE) was performed for LB medium (LB, 10 μL), IPTG induction medium (IN, 10 μL), the cell lysate supernatants with different loading volumes (S: 10, 20, 30 μL), and precipitation (P, 10 μL) to inspect the expression of ΔCaSR. A protein marker (molecular weight: 15−200 kDa) was used as a reference, and the gel (12% polyacrylamide) was stained with Coomassie blue.

2.3. Preparation and Characterization of the Immobilized ΔCaSR Stationary Phase Material. The bare silica gels were activated and further prepared as aminopropyl silica gels according to our previous protocol.[19] The aminopropyl silica gels (1.6 g) and N,N'-carbonyldiimidazole (CDI, 2.4 g) were suspended in acetonitrile (30 mL) at 25 °C and stirred for 3 h to obtain CDI-modified silica gel. Then, a benzylcytosine derivative (BC), like 2-(4-(aminomethyl)-benzyl)oxy-pyrimidin-4-amine (0.096 g), was added to the suspension of CDI-modified silica gels (1.6 g) in acetonitrile and reacted by stirring for 3 h to obtain BC-coupled silica gels. Finally, the dried BC-coupled silica gels (0.8 g) were incubated with the supernatant of cell lysates (50 mL) containing CLIP-tagged ΔCaSR at 25 °C for 30 min to obtain ΔCaSR-immobilized silica gels. The ΔCaSR-immobilized silica gels were stored in phosphate buffer (pH 7.4, 20 mM) in a refrigerator.

X-ray photoelectron spectra (PHI5000 Versa Probe III, ULVAC-PHI, INC., Japan) were acquired for the different types of silica gels to determine if ΔCaSR was trapped. SDS-PAGE was performed for LB medium (LB, 10 μL), the cell lysate supernatants before immobilization (SBI, 10 μL) and after immobilization (SAI, 10 μL), as well as the protein marker (M, 10 μL). The amount of the immobilized ΔCaSR was calculated according to the equation: $Q = (P_{SBI} \times C_{SBI} - P_{SAI} \times C_{SAI}) \times V_p/m_{silica}$. P_{SBI} and P_{SAI} were the percentages of ΔCaSR in the supernatant before and after immobilization, based on grayscale analysis of SDS-PAGE using the ImageJ software. C_{SBI} and C_{SAI} were the concentrations of the total protein in the supernatant before and after immobilization, which were measured by a bicinchoninic acid assay. V_p and m_{silica} represent the total volume of cell lysate and the mass of dried silica gels, respectively.

2.4. Evaluation of the Immobilized ΔCaSR Column. ΔCaSR-immobilized silica gels were used as stationary phase materials for packing the stainless-steel tube (4.6 × 50 mm) to obtain the immobilized ΔCaSR column. They were stored at 4 °C when not in use. The column was equipped for ion chromatography with an electrical conductivity detector (ICS6000, Thermo Fisher Scientific Inc.). Each of sodium chloride (NaCl), calcium nitrate Ca(NO$_3$)$_2$, and calcium chloride (CaCl$_2$) in Tris-HCl buffer solution was injected into the freshly prepared column, and their retention times and peak profiles were recorded. The CaCl$_2$ solution was flowed through the immobilized ΔCaSR column every week to inspect its stability. The chromatographic experiments were performed using a mobile phase of Tris-HCl (pH 7.4, 20 mM) at 25 °C at a flow rate of 0.2 mL/min with an injection volume of 20 μL.

2.5. The Ca²⁺ Binding Response to Allosteric Modulators on the Immobilized ΔCaSR Column. Frontal chromatography[20] was used to determine the direct interaction of the known allosteric modulators cinacalcet/NPS2143 with the immobilized ΔCaSR column. The column was equipped for high-performance liquid chromatography with a diode array detector (HPLC-DAD, LC-2030, Shimadzu). The mobile phase was prepared with ammonium acetate (50 mM, pH 7.4) containing either cinacalcet or NPS2143 at a series of concentrations: 0, 0.10, 0.25, 0.50, 1.00, 2.00, 4.00, and 8.00 μM. The column was equilibrated with the running mobile phase at a detection wavelength of 270 nm and a flow rate of

1.0 mL/min, and the breakthrough curves were recorded for determining the breakthrough time. Injection of each sample was performed in triplicate under the optimized conditions. The equation is $\frac{1}{m_{Lapp}} = \frac{1}{K_A m_L} \times \frac{1}{[A]} + \frac{1}{m_L}$, where K_A is the association constant of the allosteric modulator, m_L is the total moles of active binding sites, and $[A]$ is the concentration of the allosteric modulator in the mobile phase. The apparent adsorption amount m_{Lapp} was calculated according to the formula: $m_{Lapp} = (t_R - t_0) \times \nu_A[A]$, where t_R is the breakthrough time of the allosteric modulator, t_0 is the void time of the chromatographic system, ν_A is the flow rate of the mobile phase. When $\frac{1}{m_{Lapp}}$ is plotted against $\frac{1}{[A]}$, m_L is obtained from the straight-line intercept, and K_A is obtained from the straight-line slope.

Ion chromatography with an electrical conductivity detector equipped with the immobilized ΔCaSR column was flushed independently with the mobile phases of Tris-HCl (20 mM, pH 7.4) containing cinacalcet or NPS2143 at increasing concentrations of 0, 0.10, 0.25, 0.50, 1.00, 2.00, 4.00, and 8.00 μM for 1 h. Under equilibration with each mobile phase, CaCl$_2$ (4.0 mM, 10 μL) was injected into the column to monitor its retention behavior. The retention factor k' of Ca²⁺ on the column can be calculated by $k' = (t_R - t_0)/t_0$, where t_R is the retention time of the analyte and t_0 is the void time of the chromatographic system. The concentration of the allosteric modulator with the greatest influence on the retention factor k' of Ca²⁺ was defined as the optimized concentration. To quantify allosteric effects on agonist binding, the CaCl$_2$ solutions with a series of concentrations of 1.5, 2.0, 2.5, 3.0, 3.5, 4.0, 4.5, and 5.0 mM were independently injected into the column with the mobile phase of Tris-HCl (20 mM, pH 7.4) containing cinacalcet (0.50 μM) or NPS2143 (0.25 μM) at a flow rate of 0.2 mL/min with a volume of 10 μL. At the end of each series, the column was fully equilibrated using the next mobile phase (approximately 30 min). An injection amount-dependent method was used to reveal ligand–protein interaction according to the relationship between the mole amount of the injected solute and its retention factor.[21] This can be described by the equation $k'n_b/(1 + k') = m_L - \frac{1}{K_A}k'V_m$. Here, V_m is the void volume of the chromatographic system; n_b is the mole amount of one injection; m_L is the total mole of binding sites between the ligand and the protein; k' represents the retention factor; K_A denotes the association constant of the ligand bound to the protein. The linear regression curve between $k'n_b(1 + k')$ and $k'V_m$ can be constructed accordingly, and K_A and m_L can be obtained from the slope and intercept of the regression curve equation.

2.6. Screening and Identifying the Potential Allosteric Ligands from Epimedii Folium. The powder (2.0 g) of Epimedii Folium (EF), mixed with 99% methanol (20 mL) in a flask, was extracted by discontinuous ultrasonication for 30 min (1 min sonication with a 1-min break), and the extract solution was evaporated to dryness, and the dried sediments were dissolved in water to prepare the EF extract sample for analysis. Filtered through a 0.22 μm membrane, three aliquots (10.0 μL) of the EF extract were analyzed at 25 °C under a detection wavelength of 270 nm using HPLC-DAD (LC-2030, Shimadzu). One aliquot was injected into an Agilent TC-C18 column (4.6 × 250 mm, 5 μm) for analyzing chemical compositions with a mobile phase consisting of acetonitrile
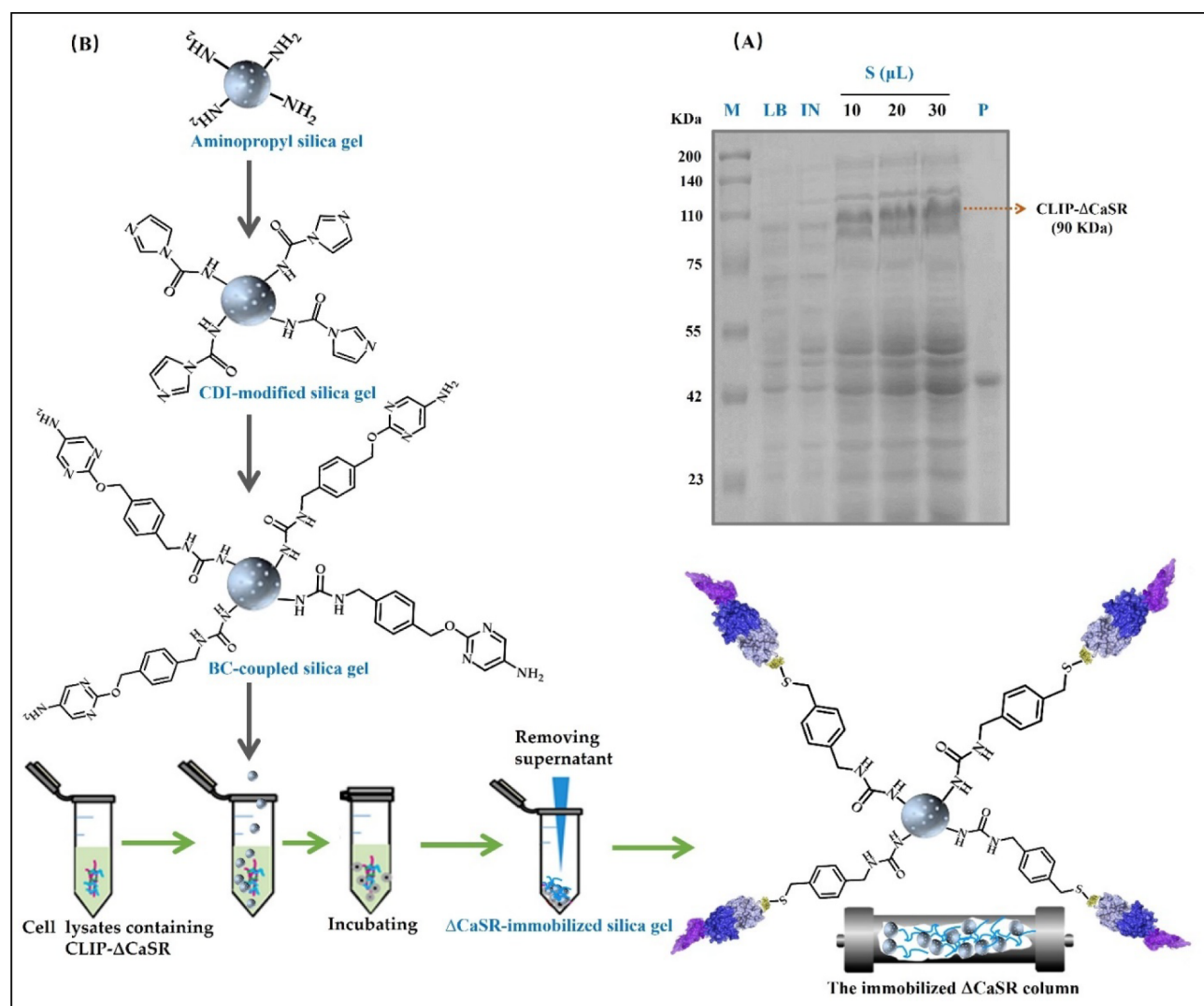
Figure 1. Schematic overview of the preparation process of the immobilized ΔCaSR column. (A) The SDS-PAGE analysis for the expression of CLIP-tagged ΔCaSR in *E. coli* cells (Lane M: protein marker, Lane LB: Luria–Bertani medium; Lane IN: IPTG induction medium, Lane S: different loading volumes (10, 20, 30 μL) of the supernatant of cell lysates; Land P: precipitation of cell lysates). (B) The immobilized ΔCaSR column was packed with ΔCaSR-immobilized silica gel, which was prepared from aminopropyl silica gel, CDI-modified silica gel, to BC-coupled silica gel.

(A) and water containing 0.1% formic acid (B) at a step gradient (0–25 min: 25% A; 25–40 min: 30% A; 40–55 min: 41% A; 55–70 min: 52% A) with a flow rate of 1.0 mL/min. The other two aliquots were injected into the immobilized ΔCaSR column and the control column (the used column with denatured ΔCaSR), respectively, with a mobile phase of ammonium acetate (pH 7.4, 50 mM) at a flow rate of 1.0 mL/min. The peaks were regarded as the binders if their retention times were longer than the void time of the chromatographic system, and they were collected manually and condensed for HPLC-MS analysis (LCMS-8045, Shimadzu). Liquid chromatography separation was performed on an Agilent XDB-C18 column (2.1 mm × 50 mm, 1.7 μm) with a mobile phase of acetonitrile (A) and water containing 0.1% formic acid (B) (55/45, V_A/V_B) at a flow rate of 0.3 mL/min and an injection volume of 5 μL. Mass spectrometric detection was conducted using a triple quadrupole tandem mass spectrometer equipped with an electrospray ionization (ESI) interface in the negative ion mode. The optimal ESI-source operation parameters were set as follows: capillary voltage of 5.5 kV, declustering potential

of 40 V, and collision energy of 10 eV. The temperatures of the heating block, desolvation line, and drying gas were 400, 526, and 400 °C, respectively. The nebulizing gas and drying gas flow rates were 3 and 10 L/min, respectively. MS and MS/MS data were acquired in a scan range between 50 and 1500 Da and processed using the installed software package.

2.7. Competitive Study of the Screened Compounds with Allosteric Modulators. A competitive study was conducted to test the allosteric binding of the screened compounds within ΔCaSR. Ammonium acetate solutions (pH 7.4, 50 mM) containing cinacalcet or NPS2143 at concentrations of 0, 0.10, 0.25, 0.50, 1.00, 2.00, 4.00, and 8.00 μM were used as the running buffers. The breakthrough curves were recorded using HPLC-DAD until a steady platform was achieved. At this moment, the aqueous solutions of the screened compounds (1.0 mM, 5 μL), including epimedin B, epimedin C, and icariin, were independently injected into the immobilized ΔCaSR column to monitor their retention behaviors.

2.8. Verifying the Allosteric Effect of the Screened Compounds on MC3T3-E1 Cells. The murine osteoblastic cell line MC3T3-E1 was obtained from the Cell Bank of the Chinese Academy of Sciences (Shanghai, China). The cells were cultured in α-MEM supplemented with 10% fetal bovine serum and 1% each of penicillin and streptomycin. The culture medium was changed every 2 days. MC3T3-E1 cells (10 000 cells/well) were plated in 96-well plates in α-MEM and incubated at 37 °C under a humidified atmosphere of 5% CO_2 and 95% air. After 12 h, the cells were treated with $CaCl_2$ solutions at different concentrations of 0, 0.1, 0.25, 0.50, 1.0, 2.0, 4.0, and 8.0 mM for 24 h, while the control cells were administered α-MEM. Solutions of cinacalcet, NPS2143, epimedin B, epimedin C, and icariin with a series of concentrations at 0, 2.5, 5.0, 10, 20, 40, 80, and 120 μM were prepared in α-MEM media containing 4 mM $CaCl_2$ for treating the cells. Cell Counting Kit-8 (10 μL) was added to each well and incubated for 1.5 h. After that, an MTT assay was performed at 450 nm, and cell viability (%) was calculated according to the formula: absorbance of the treated cells/absorbance of the control cells × 100%.

For the intracellular Ca^{2+} measurement, MC3T3-E1 cells (10 000 cells/well) were plated in 96-well plates in α-MEM media and incubated for 24 h at 37 °C under a humidified atmosphere of 5% CO_2 and 95% air. The seven groups of cells were treated with 4 mM $CaCl_2$, 5 μM cinacalcet + 4 mM $CaCl_2$, 3.2 μM NPS2143 + 4 mM $CaCl_2$, 2.5 μM epimedin B + 4 mM $CaCl_2$, 2.5 μM epimedin C + 4 mM $CaCl_2$, and 5 μM icariin + 4 mM $CaCl_2$ for 24 h, while the control cells were maintained in the α-MEM medium without any treatment. The cells were washed with PBS after the removal of the culture solution, and then Fluo-4 AM (0.5 μM, 100 μL) was added and incubated for 0.5 h to measure Ca^{2+} release. Fluorescence was detected in each well continuously with Flash SuPerMax 3100 (Shanghai, China) at 490 nm excitation and 525 nm emission. Relative peak fluorescence units were normalized to the fluorescence observed in the absence of Ca^{2+} and the ligands (control group). For the cAMP assay, the treated cells were lysed by repeated freeze/thaw cycles after the addition of 100 μL RIPA and centrifuged to remove cell debris. The supernatant was measured using the cAMP parameter immunoassay kit according to the manufacturer's instructions. OD values were measured at 405 nm using a multifunctional microplate reader, and cAMP concentration was calculated based on the standard curve. Data ($n = 3$) were presented as mean ± RSD, and statistical analysis was performed by one-way ANOVA using the GraphPad prism 8.0 software package. Intergroup differences were considered significant at *$p < 0.05$, **$p < 0.01$, ***$p < 0.001$ vs the group treated with $CaCl_2$.

3. RESULTS AND DISCUSSION

3.1. Preparation of the Immobilized ΔCaSR Stationary Phase Material. Figure 1A displays the SDS-PAGE image, where a target band close to 110 kDa in the protein marker (M) does not appear in either the Luria−Bertani medium (LB) or the precipitation (P) but emerges in the IPTG induction medium (IN) and the supernatants of cell lysates (S). This band was attributable to CLIP-ΔCaSR since the molecular weight of ~90 kDa is the sum of the extracellular domain-deleted CaSR (ECD-deleted CaSR, ΔCaSR, ~70 kDa) and the CLIP-tag (20.0 kDa). Also, it can be seen that the expression levels of CLIP-ΔCaSR are dependent on the sample-loading volumes of supernatants, suggesting that the

recombinant CaSR is located in the soluble fraction of the cell lysates. Our work demonstrated that the fused ΔCaSR with the CLIP-tag was successfully expressed in *E. coli* cells. Figure 1B indicates the workflow for preparing the ΔCaSR-immobilized silica gels, starting from aminopropyl silica gel and CDI-modified silica gel to BC-coupled silica gel as stationary phase materials for column packing. ΔCaSR-immobilized silica gels were synthesized through a site-specific covalent reaction between the CLIP-tag moiety and the benzylcytosine derivative substrate on the BC-coupled silica gels. This immobilization method has been proven feasible in our previous study.[22] Different from the immobilization techniques requiring the purified protein solution to prevent interference from other competing proteins, the benzylcytosine derivative shows no significant reactivity against proteins other than the CLIP tag (DNA repair protein O[6]-alkylguanine-DNA alkyltransferase),[23] enabling the immobilization of the CLIP-fused protein directly from cell lysates without the need for complicated purification steps. The site-specific immobilization using affinity tags represents a new way of combining purification and immobilization in a one-step procedure, simplifying the synthesis of ΔCaSR-based stationary phase materials with many advantages, such as time and cost savings, as well as minimal activity loss of the protein.

3.2. Characterization of the Immobilized ΔCaSR Stationary Phase Material. X-ray photoelectron spectra for the different types of silica gels show several peaks at 103, 286, 399, and 533 eV (Figure 2A), which are assigned to the corresponding elements of silicon (Si), carbon (C), nitrogen (N), and oxygen (O). The graph of elemental distribution (Figure 2B) indicates the percent contents of the four elements on the different silica gels, including bare silica gel (a), aminopropyl silica gel (b), CDI-modified silica gel (c), BC-coupled silica gel (d), and ΔCaSR-immobilized silica gel (e). Compared with BC-coupled silica gel (before immobilization), a 1.4-fold and 1.5-fold increase in carbon and nitrogen (representatives of CaSR), as well as a 1.3-fold and 1.6-fold reduction in silicon and oxygen (representatives of SiO_2 particles), were presented on ΔCaSR-immobilized silica gel (after immobilization). This is rational since the protein contains a carbon skeleton and many peptide bonds. In addition, the SDS-PAGE image shows that the grayscale of target bands (~90 kDa in Figure 2C) becomes faded in the supernatant after immobilization (SAI) in comparison with before immobilization (SBI), confirming that ΔCaSR was integrated onto the supports. It was noted that some other bands appear less intense after immobilization, which is most likely due to the physical adsorption of other competing proteins on silica gel. To avoid errors, the SDS-PAGE images ($n = 3$) were used to determine the immobilization amount of ΔCaSR. Based on grayscale analysis, P_{SBI} 3.89% for ΔCaSR in the supernatants before immobilization decreased to P_{SAI} 3.63% after immobilization. Meanwhile, the total protein concentrations in the cell lysate supernatants were calculated as C_{SBI} 4.39 mg/mL before immobilization and C_{SAI} 1.93 mg/mL after immobilization. When the BC-coupled silica gels ($m_{silica} = 1.20$ g) were incubated in the supernatant ($V_p = 50$ mL), the immobilization amounts were calculated as 4.2 mg of ΔCaSR per gram of silica gel according to the equation of $Q = (P_{SBI} \times C_{SBI} - P_{SAI} \times C_{SAI}) \times V_p/m_{silica}$. This was generally consistent with previous data for CaSR immobilized on chloroalkane-modified silica gels when the Halo-tag was fused
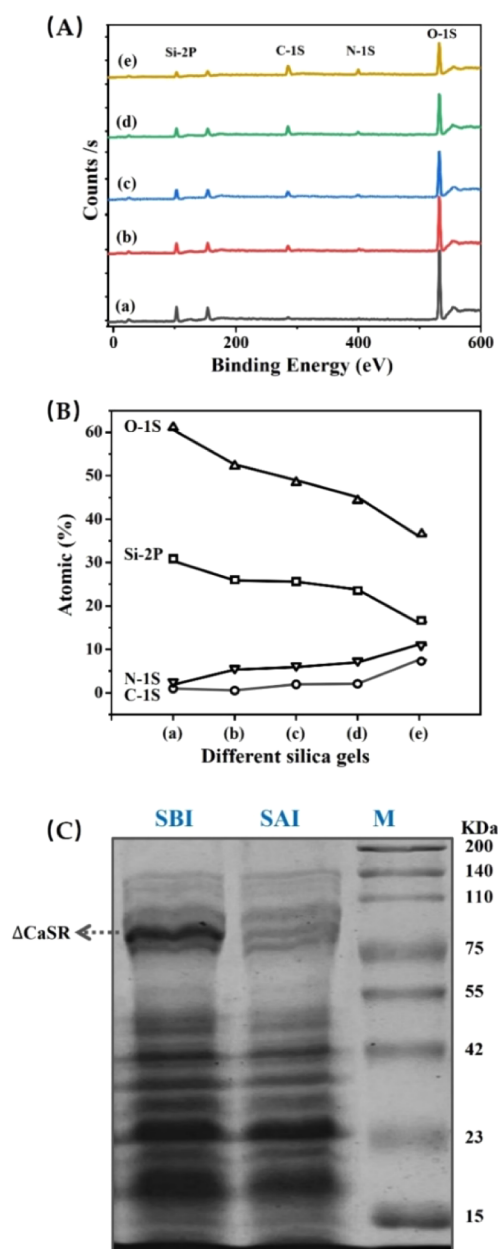
Figure 2. Characterization of the immobilized ΔCaSR stationary phase material using X-ray photoelectron spectroscopy (A) and the graph of elemental distribution (B) for bare silica gel (a), aminopropyl silica gel (b), CDI-modified silica gel (c), BC-coupled silica gel (d), and ΔCaSR-immobilized silica gel (e). SDS-PAGE (C) was used to determine the immobilization amount of ΔCaSR on the stationary phase material (Lane SBI: the supernatant of cell lysates before immobilization, Lane SAI: the supernatant of cell lysates after immobilization, and Lane M: protein marker).

to the N-terminal extracellular domain of CaSR.[24,25] In this case, such an immobilization amount can meet the requirements for screening allosteric ligands in the following experiments.

3.3. Evaluating Ligand-Recognition Activity and Stability of the Immobilized ΔCaSR Column.

CaSR is activated by the endogenous ligand Ca^{2+}, and herein, the $CaCl_2$ and $Ca(NO_3)_2$ solutions were used to evaluate the ligand-recognized activity of the immobilized ΔCaSR column using ion chromatography with an electrical conductivity detector.

Different from only one peak observed for Na^+/Cl^- in the NaCl solution, two separate peaks in $CaCl_2$ and $Ca(NO_3)_2$ were observed on the immobilized ΔCaSR column (Figure 3A). It is clear that cations exhibit a much longer retention time ($Ca^{2+} = \sim4.5$ min) than anions ($NO_3^- = \sim2.6$ min, $Cl^- = \sim2.3$ min), suggesting that the immobilized ECD-deleted CaSR is capable of recognizing its agonist, Ca^{2+}. Interestingly, Ca^{2+} was retained on the immobilized ΔCaSR column, leading us to presume that additional binding sites for Ca^{2+} were present in the 7-transmembrane domain (7TMD) of CaSR. This can be understood by the fact that Ca^{2+} was able to activate CaSR even when the entire extracellular domain was inaccessible, with the extracellular region arising from the exoloops in the 7TMD.[10,26] The stability of the column was inspected repeatedly with $CaCl_2$ as a probe over a period of 4 weeks. As shown in Figure 3B, the approximate retention times and the virtually identical peak profiles of $CaCl_2$ are during the first week, the second week, and the third week, but a noticeable change appears at the fourth week, indicating that the column remains stable within 3 weeks. Together, we reason that the immobilized ΔCaSR column exhibits ligand-recognition activity and maintains comparable stability to other receptor immobilization systems with a 3-week stability.

3.4. The Ca^{2+} Binding Response to Allosteric Modulators on the Immobilized ΔCaSR Column.

Frontal chromatography was used to explore the direct interaction of allosteric modulators with the immobilized ΔCaSR, in which the saturation of the column with the continuous infusion of allosteric modulators results in a series of breakthrough curves, and the association equilibrium constants of the allosteric modulator can be obtained. The mobile phases containing the increasing concentrations of cinacalcet (Figure 4A1) or NPS2143 (Figure 4B1) ran through the immobilized ΔCaSR column. The chromatographic elution profiles (breakthrough curves) with the front and plateau regions suggested that the allosteric sites of ΔCaSR became fully occupied with cinacalcet or NPS2143 when a steady platform was achieved. The profiles shifted forward in a concentration-dependent manner, namely, the breakthrough times became shortened, reflecting that the occupancy of allosteric sites within ΔCaSR was related to the amounts of allosteric modulator. Reciprocal linear regression of the apparent adsorption amount versus the concentration of the allosteric modulator (Figure 4C1) was used to predict the association constant K_A and the total mole of binding sites m_L (Table 1). The K_A values of 5.24×10^5 M^{-1} for cinacalcet and 4.51×10^5 M^{-1} for NPS2143 indicated that the removal of the CaSR extracellular domain does not prevent allosteric ligands from acting directly on the 7-transmembrane domain. This phenomenon was evidenced by the finding that allosteric binding sites within the 7-transmembrane domain came from the N-terminally truncated CaSR.[27] Therefore, ECD-deleted CaSR retained the binding activity of allosteric modulators.

To understand the allosteric effect on agonist binding, the retention behaviors of the agonist Ca^{2+} on the immobilized ΔCaSR column were monitored when an allosteric modulator was present in the mobile phase at the concentrations ranging from 0 to 8.00 μM. The overlapping chromatograms displayed that the retention times of Ca^{2+} had been altered by cinacalcet (Figure 4A2) or NPS2143 (Figure 4B2) in a concentration-dependent manner, but the Cl^- peak positions remained unchanged. We plotted the retention factor k' of Ca^{2+} versus the concentration of the allosteric modulator in the mobile phase (Figure 4C2), revealing that the inflection points of Ca^{2+}
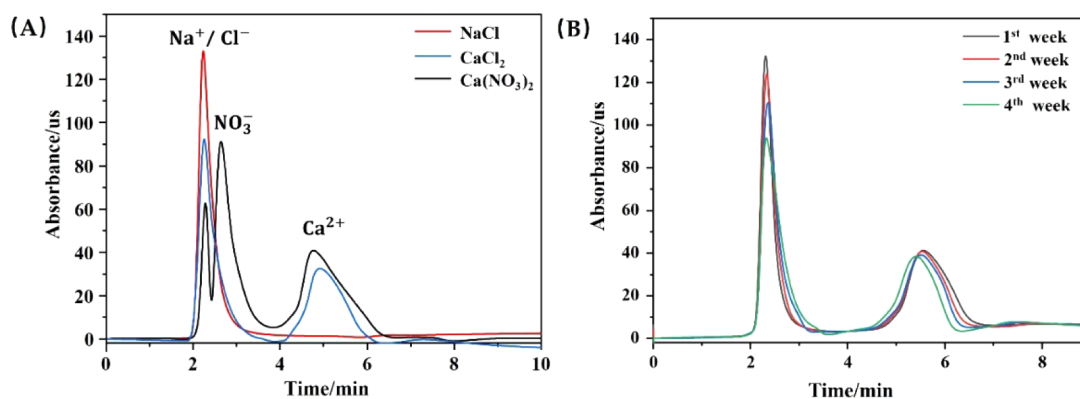
Figure 3. Evaluating ligand-recognized activity and stability of the immobilized ΔCaSR column using ion chromatography with an electrical conductivity detector. (A) The overlapping chromatograms of sodium chloride (NaCl), calcium chloride (CaCl$_2$), and calcium nitrate (Ca(NO$_3$)$_2$) in Tris-HCl buffer solution. (B) The chromatography of CaCl$_2$ at different time points.
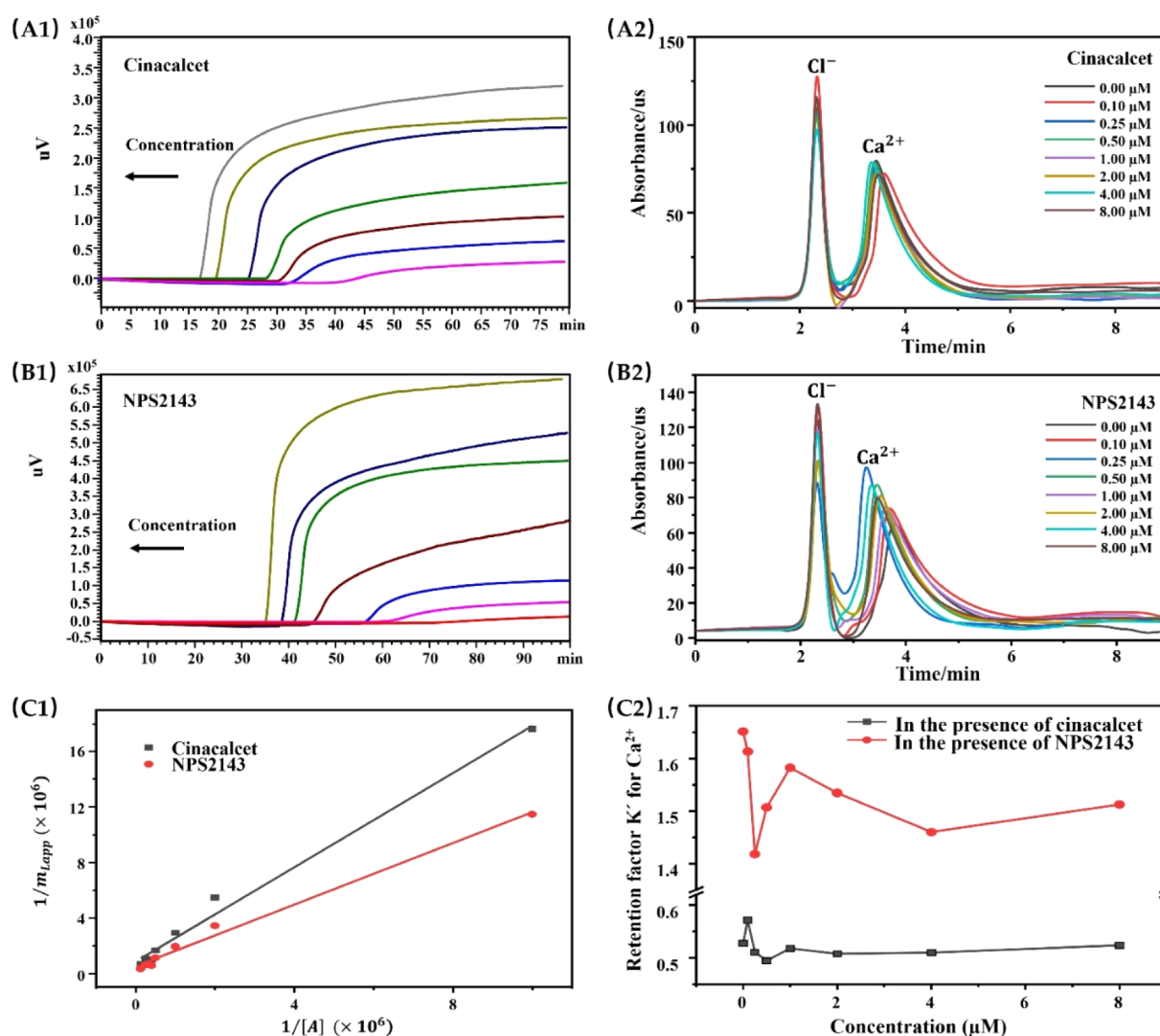

Figure 4. Mobile phases containing increasing concentrations of cinacalcet (A1) or NPS2143 (B1) were run through the immobilized ΔCaSR column, and CaCl$_2$ (4.0 mM) was injected under equilibration with the mobile phases containing increasing concentrations of cinacalcet (A2) or NPS2143 (B2). Reciprocal linear regression of the apparent adsorption amount versus the concentration of cinacalcet or NPS2143 predicted the binding parameters of cinacalcet or NPS2143 (C1). The retention factor (k') of Ca^{2+} versus the concentration of cinacalcet or NPS2143 (C2). The increasing concentrations of cinacalcet or NPS2143 were given as 0.10, 0.25, 0.50, 1.00, 2.00, 4.00, and 8.00 μM.

binding emerged at 0.50 μM for cinacalcet and at 0.25 μM for NPS2143. The emergence of these inflection points can be

taken as evidence that they induced the greatest allosteric conformational change of the immobilized receptor. Normally,

Table 1. Binding Parameters for Allosteric Modulators and Agonist Ca²⁺ on the Immobilized ΔCaSR Column

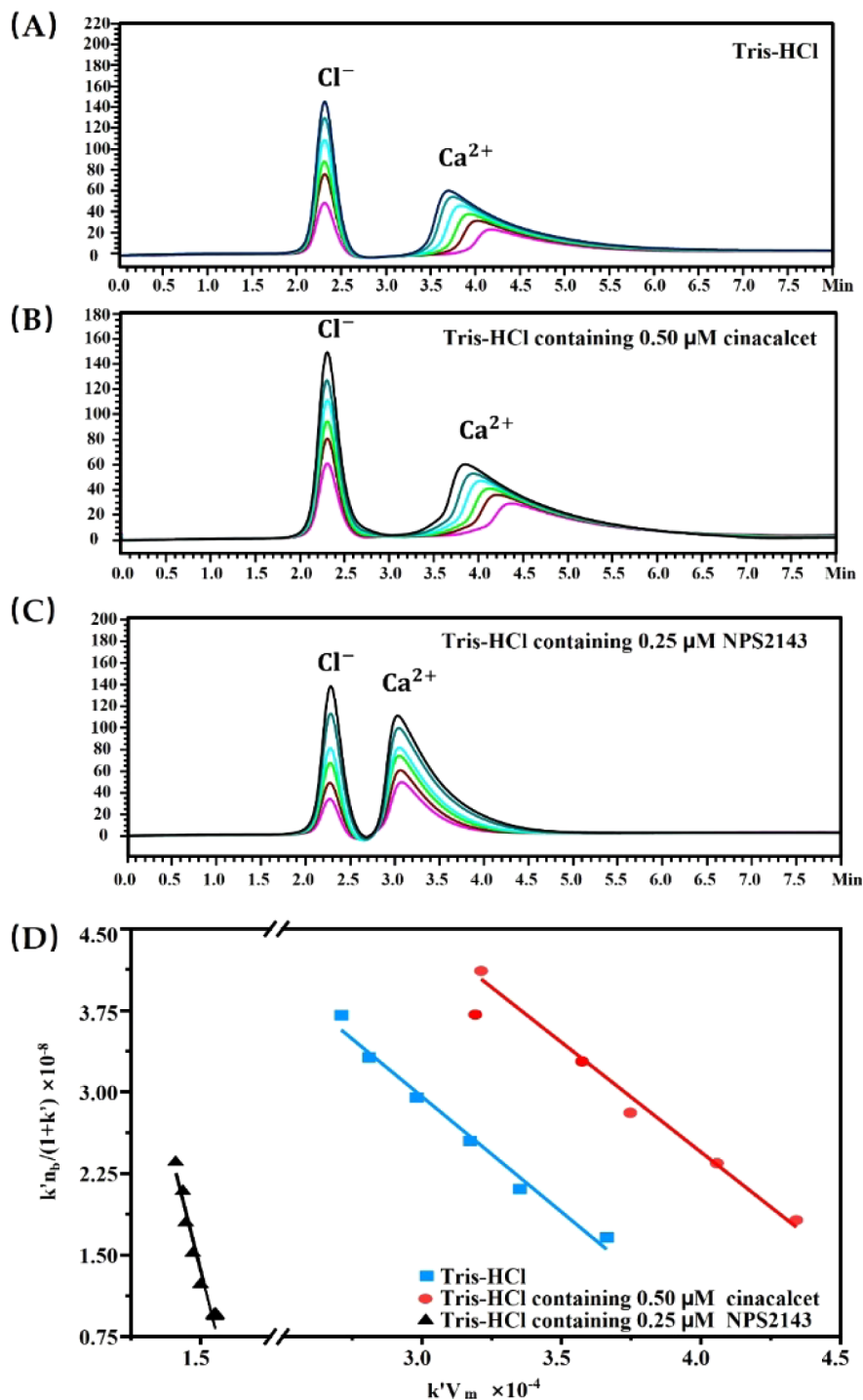| Mobile phase	Cinacalcet		NPS2143		Ca²⁺	
	K_A (M⁻¹) × 10⁵	m_L (mol) × 10⁻⁷	K_A (M⁻¹) × 10⁵	m_L (mol) × 10⁻⁷	K_A (M⁻¹) × 10³	m_L (mol) × 10⁻⁷
buffer	5.24 ± 1.43	1.12 ± 0.28	4.51 ± 0.08	1.88 ± 0.07	4.73 ± 0.31	0.93 ± 0.04
buffer + 0.50 μM cinacalcet					5.12 ± 0.26	1.04 ± 0.04
buffer + 0.25 μM NPS2143					1.10 ± 0.11	1.66 ± 0.17

Figure 5. Overlapping chromatograms of CaCl₂ in the increasing concentrations of 1.5, 2.0, 2.5, 3.0, 3.5, 4.0, 4.5, and 5.0 mM were presented on an ΔCaSR-based column in the mobile phases of Tris-HCl (A), Tris-HCl containing 0.50 μM cinacalcet (B), and Tris-HCl containing 0.25 μM NPS2143 (C). The curves were fitted using the equation of $k'n_b/(1 + k') = m_L - \frac{1}{K_A}k'V_m$ (D) based on the injection amount-dependent method.
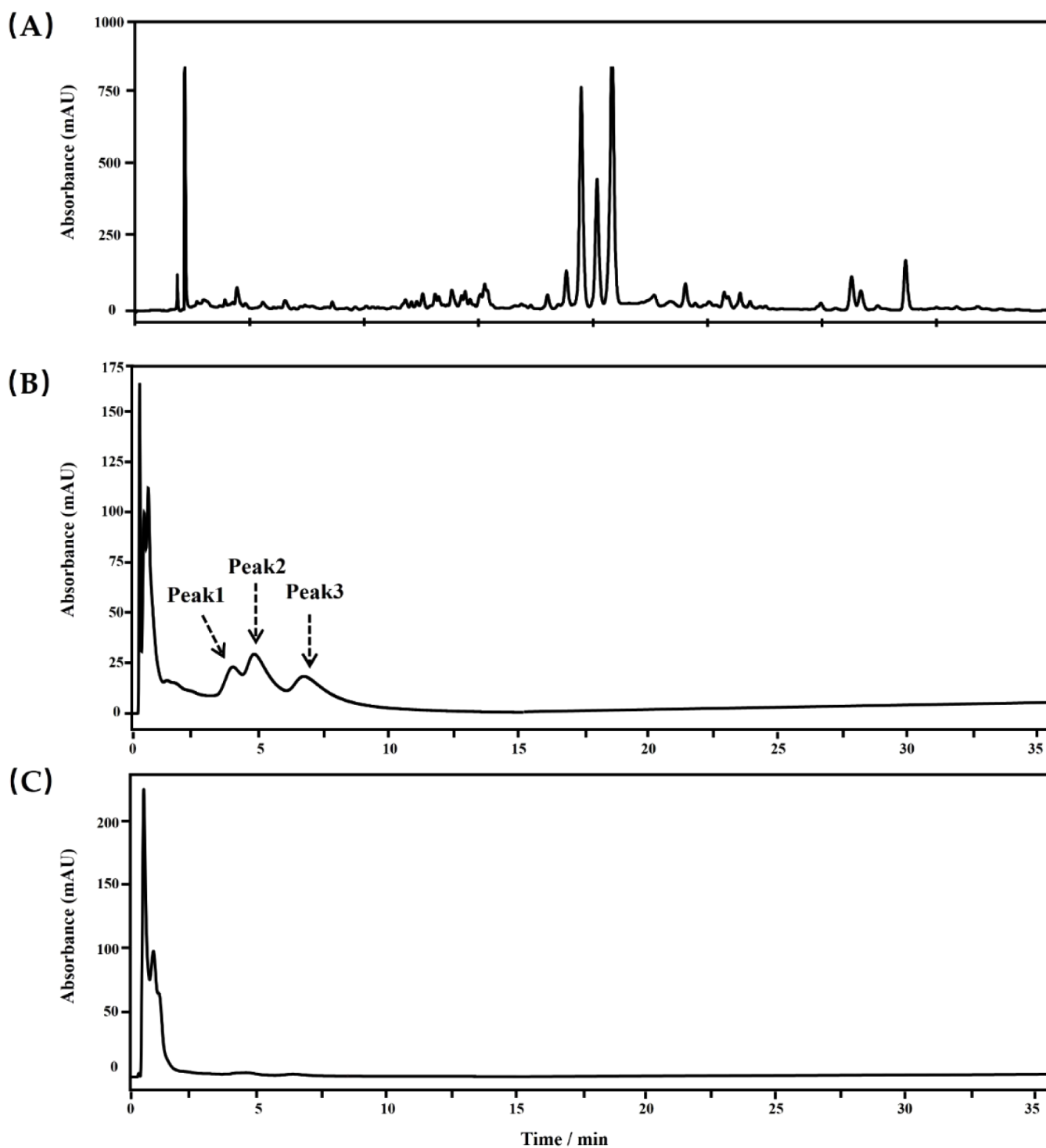
Figure 6. Three aliquots of the Epimedii Folium (EF) extract were flowed through the Agilent TC C18 column (A), the immobilized ΔCaSR column (B), and the control column (C) in HPLC-DAD, respectively.

the CaSR complexed with Ca^{2+} and cinacalcet represents the positive allosteric modulating state, while CaSR in complex with Ca^{2+} and NPS2143 represents the negative allosteric modulating state, where the conformational plasticity of CaSR has been demonstrated using cryo-electron microscopy.[28] The results of our study proved that the immobilized ECD-deleted CaSR exhibited the Ca^{2+} binding response to the different allosteric states of the receptor, and the greatest allosteric response occurred at 0.50 μM for cinacalcet and at 0.25 μM for NPS2143. Although the exact conformational dynamics of the

immobilized ΔCaSR in the column remain unknown, this does not affect the separation of nonbinders and binders on the immobilized ΔCaSR. Our further work can be conducted to characterize the conformational dynamics of the immobilized receptor using additional biophysical methods such as circular dichroism and NMR spectroscopy.

To quantify the allosteric effect on the binding affinity of Ca^{2+}, the injection amount-dependent method was used when the $CaCl_2$ solutions were injected after the saturation of the column with allosteric modulators. The overlapping chromato-
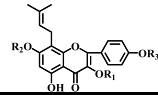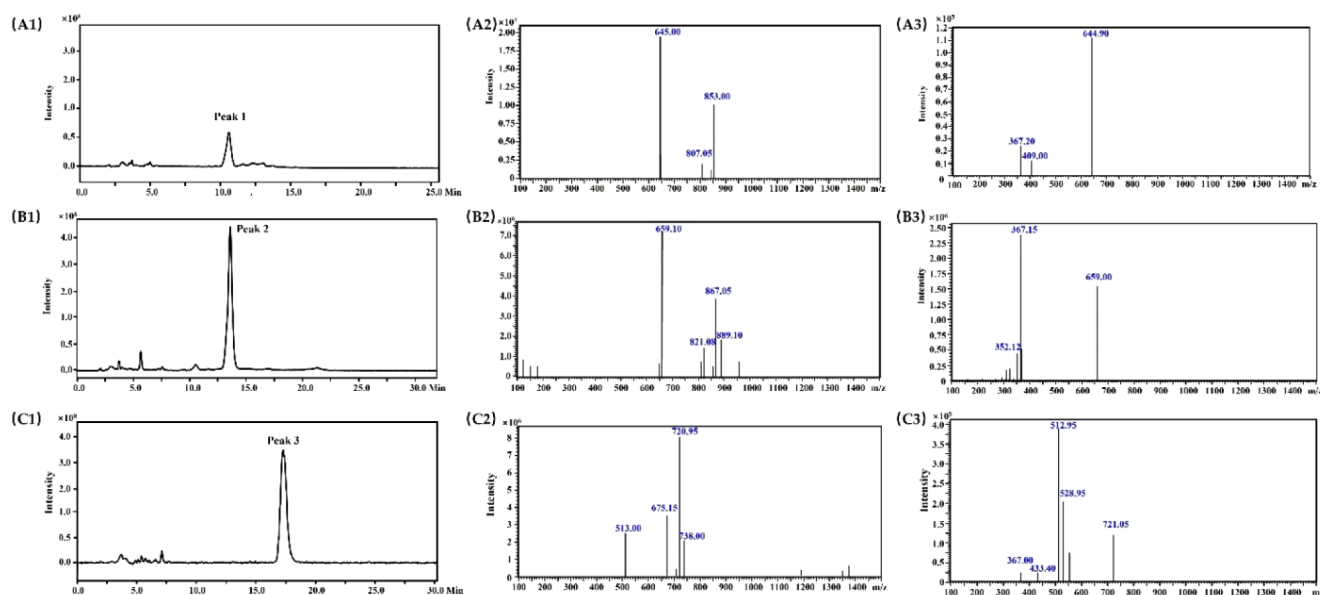
Figure 7. Elute collections from the immobilized ΔCaSR column were analyzed using HPLC-MS, providing the total ion current chromatogram, mass spectrum, and MS/MS for Peak1 collection (A1−A3), Peak2 collection (B1−B3), and Peak3 collection (C1−C3).

Table 2. Screened Compounds from the Epimedii Folium Extract Using the Immobilized ΔCaSR Column

	MS m/z	MS/MS m/z	MW	Compound	R1	R2	R3
Peak1	853.00, 807.05	644.90, 367.20	808.776	Epimedin B	Rha-Xyl	Glu	CH_3
Peak2	867.05, 821.08	659.00, 367.15, 352.10	822.803	Epimedin C	Rha-Rha	Glu	CH_3
Peak3	720.95⁻, 675.15	513.05, 528.95, 367.00	676.662	Icariin	Rha	Glu	CH_3

grams of the $CaCl_2$ solutions with increasing injection amounts are shown in the absence (Figure 5A) and the presence of 0.50 μM cinacalcet (Figure 5B) or 0.25 μM NPS2143 (Figure 5C) on the immobilized ΔCaSR column in ion chromatography with an electrical conductivity detector. Compared with the immovable peak position of Cl^-, the retention times of Ca^{2+} gradually shortened with the increasing injection amount. The fitted curves, according to the equation $k'n_b/(1 + k') = m_L - \frac{1}{K_A}k'V_m$, provided the association equilibrium constant K_A and the total moles of active binding sites m_L (Table 1). In the absence of an allosteric modulator, the K_A of Ca^{2+} was 4.73×10^3 M^{-1}, which was roughly in line with the binding affinity of Ca^{2+} in the reported study.[29] In the presence of an allosteric modulator, cinacalcet-induced K_A increase was 8% for Ca^{2+} but NPS2143-induced K_A reduction was 77%, compared with the data from the absence of an allosteric modulator. This is rational since cinacalcet, as a positive allosteric modulator, increases the binding affinity of the agonist Ca^{2+}, whereas NPS2143 as a negative allosteric modulator has the opposite effect.[30] It was attributed that positive and negative modulators induced distinct conformational changes of the receptor, which subsequently led to different binding affinities for Ca^{2+}. Even so, the total binding sites of m_L for Ca^{2+} were not obviously altered by cinacalcet or NPS2143, which indicated that the ECD-deleted CaSR truncation retained enough active binding sites. This result can be sustained from the accumulated evidences that Ca^{2+}

interacted with four binding sites in the Venus Flytrap domain of the ECD[31,32] and two or more sites in the 7TMD.[11,33] Our observations provided convincing proof that the immobilized ΔCaSR column has an allosteric effect on the binding affinity of the agonist Ca^{2+}.

3.5. Screening and Identifying Allosteric Ligands from Epimedii Folium. Epimedii Folium (EF) was clinically prescribed as a water decoction for the prevention and treatment of osteoporosis in China, suggesting that the hydrophilic compounds in EF play a vital role in treating diseases. Hence, the hydrophilic molecules were preferred for investigation in this work. Methanol was selected as the solvent because it can extract the vast majority of hydrophilic compounds and a small quantity of lipophilic ones from herbs. As shown in Figure 6A, over 50 peaks were presented in the chromatogram of the EF extract on the Agilent TC C18 column, indicating the presence of complicated chemical constituents. When the EF extract was flowed through the immobilized ΔCaSR column (Figure 6B), the presence of several broad peaks indicated that chemical compounds were classified by their binding affinities to the receptor. By contrast, when the EF extract was run on the control column, which was derived from the used column with the denatured ΔCaSR protein, several unresolved peaks with very short retention times were presented in Figure 6C, suggesting no specific binders on the control column. The three broad peaks (Peak1, Peak2, Peak3), longer than the void time (0.5 min), represented some compounds that interacted strongly with
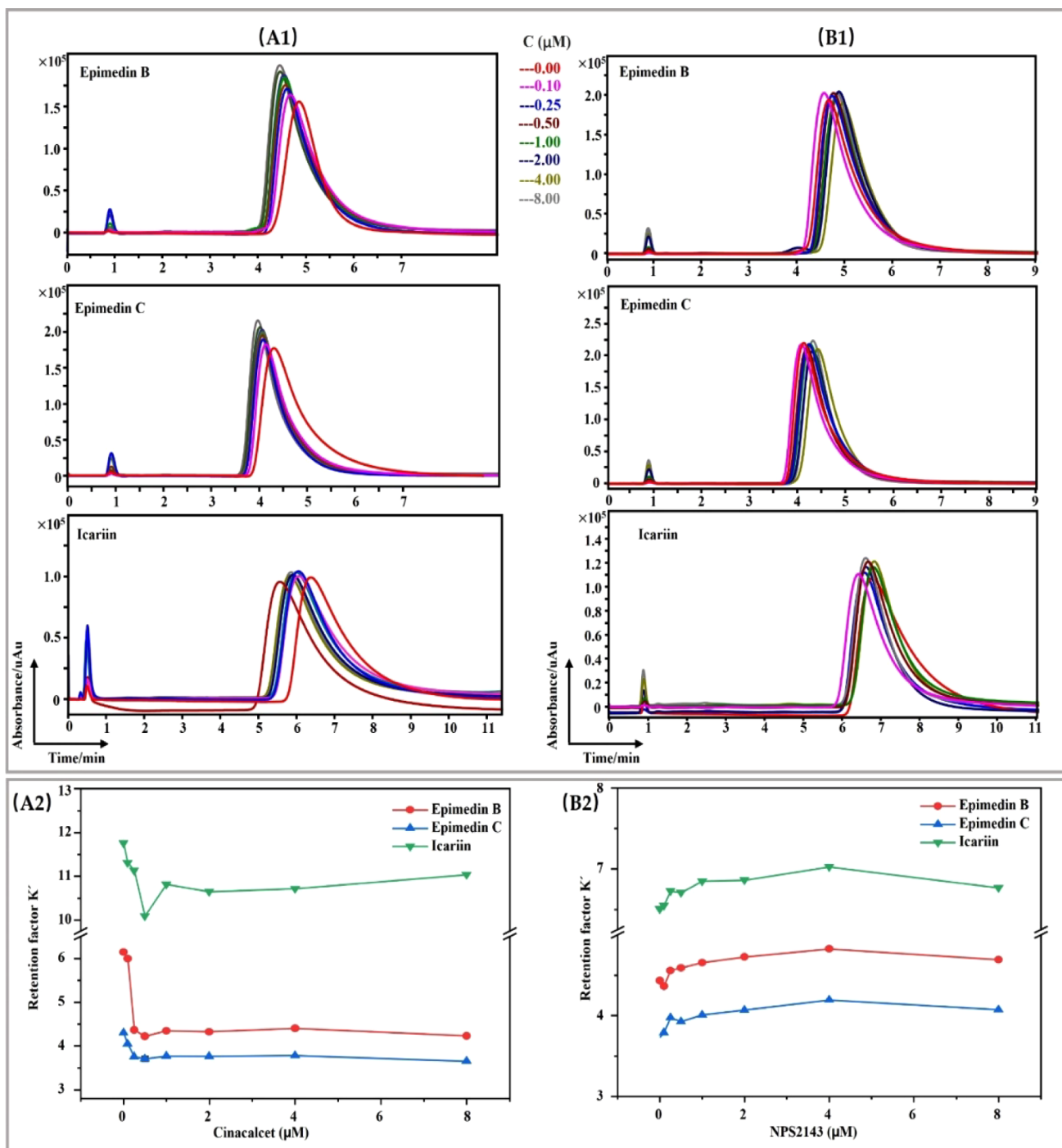
Figure 8. Screened compounds including epimedin B, epimedin C, and icariin were independently injected into the immobilized ΔCaSR column with the mobile phase containing the increasing concentrations of cinacalcet (A1) or NPS2143 (B1) at 0, 0.10, 0.25, 0.50, 1.00, 2.00, 4.00, and 8.00 μM. The retention factor (k') of the three ones changed with the concentrations of cinacalcet (A2) or NPS2143 (B2).

the ECD-deleted CaSR. The eluents from the broad peak regions were collected manually and analyzed further using HPLC-MS.

The total ion current chromatogram (TIC) and mass spectrum (MS and MS/MS) in the negative ion mode are shown in Figure 7, and the data are listed in Table 2. Only one peak appeared in the TIC of Peak1 (Figure 7A1), Peak2 (Figure 7B1), and Peak3 (Figure 7C1), indicating a pure substance in the eluent collection. The mass spectra for Peak1 (Figure 7A2,A3) showed four characteristic ions at m/z 853.00, 807.05, 644.90, and 367.20, which were consistent with

those of the standard compound Epimedin B. The deprotonated molecular ion at m/z 807.05 $[M − H]^-$ gains a HCOOH group to form an adduct ion at m/z 853.00 $[M+HCOOH−H]^-$, and it loses a glucose residue to produce a fragment peak at m/z 644.90 $[M−Glu−H]^-$ and sequentially loses rhamnose and xylose residues to generate the fragment peak at m/z 367.20 $[M−Glu−Rha−Xyl−H]^-$. As for Peak2, a molecular ion at m/z 821.08 $[M − H]^-$ and an adduct ion at m/z 867.05 $[M+HCOOH−H]^-$ were presented in the MS (Figure 7B2), and then the major fragment ions were observed at m/z 659.00 $[M−Glu−H]^-$, 367.15 $[M−Glu−Rha−Rha−$
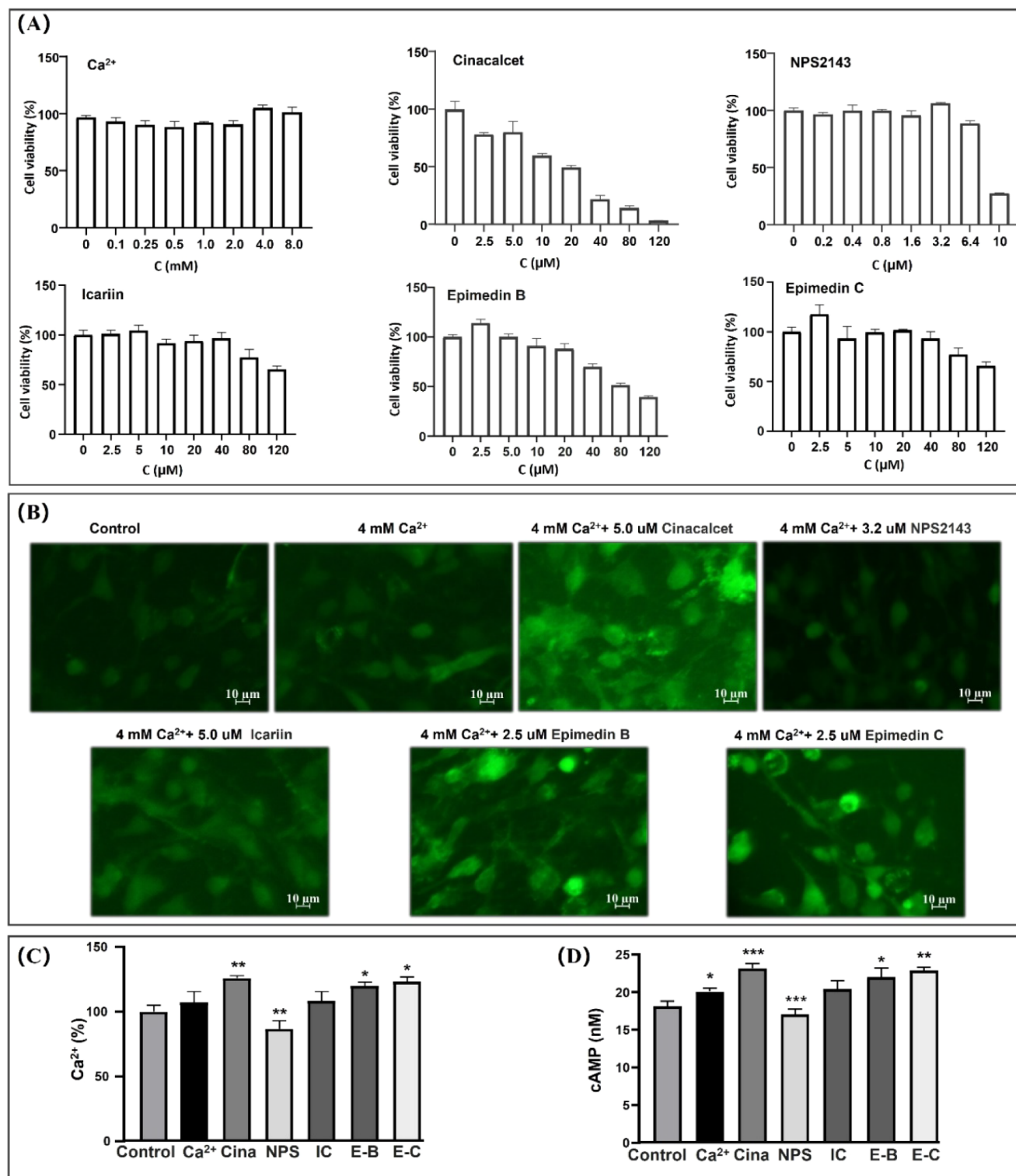
Figure 9. Allosteric effects of the screened compounds on CaSR downstream signaling in MC3T3-E1 cells were testified. (A) Cell viability (% of control) was obtained when the cells were treated with the increasing Ca^{2+} and the increasing cinacalcet, NPS2143, icariin, epimedin B, and epimedin C in the presence of 4 mM $CaCl_2$. (B) Intracellular Fluo-4 fluorescence was measured for different groups of cells. (C) The intracellular Ca^{2+} levels were calculated for different group cells. (D) Intracellular cAMP levels were measured for different group cells. Different groups were treated with α-MEM medium (Control), $CaCl_2$ (Ca^{2+}), cinacalcet (Cina), NPS2143 (NPS), icariin (IC), epimedin B (E-B), and epimedin C (E-C). Intergroup differences were considered to be significant at *$p < 0.05$, **$p < 0.01$, ***$p < 0.001$ vs the treated group with $CaCl_2$.

$H]^-$ and 352.10 $[M−Glu−Rha−Rha−CH_3−H]^-$ in the MS/ MS (Figure 7B3). The fragmentation pattern of Peak2 was consistent with the characteristics of epimedin C. In the MS of Peak3 (Figure 7C2), a fragment ion at m/z 513.00 $[M−Glu−$

$H]^-$ is produced by the loss of 162 Da (glucose residue) from the molecular ion $[M − H]^-$ at m/z 675.15, and an adduct ion $[M+HCOOH−H]^-$ at m/z 720.95 is produced by the addition of a neutral formic acid molecule (46 Da), by which icariin was

identified. This was confirmed by the characteristic ion peaks at m/z 512.95 [M−Glu−H]⁻, 528.95 [M−Rha−H]⁻, and 367.00 [M−Glu−Rha−H]⁻ in the MS/MS (Figure 7C3). In combination with the previously reported data,[34−36] Peak1, Peak2, and Peak3 were identified as epimedin B, epimedin C, and icariin from the EF extract, respectively. Although the screened compounds, belonging to prenyl flavonoid glycosides, have been proven to have antiosteoporosis effects and protect bone health in cellular, animal, and clinical studies,[37,38] this is the first time it has been found that these three compounds with therapeutic potential have the binding activity toward CaSR.

3.6. Testifying Allosteric Binding of the Screened Compounds.
To testify whether allosteric binding occurred within the 7-transmembrane domain of CaSR, we performed competition binding experiments between allosteric modulators and the screened compounds. Epimedin B, epimedin C, and icariin were independently injected and flowed through the immobilized ΔCaSR column in HPLC-DAD when cinacalcet (Figure 8A1) or NPS2143 (Figure 8B1) was included in the running mobile phase. The peaks of the three compounds shifted to different degrees in response to the varied concentrations of allosteric modulators, suggesting competitive displacement between them. To provide clarity, the retention factors k' of the three ones were calculated as illustrated in Figure 8A2,B2. It can be seen that the retention behaviors of epimedin B, epimedin C, and icariin exhibited a similar trend in a concentration-dependent fashion, and the inflection points occurred with the mobile phase containing 0.50 μM cinacalcet. When NPS2143 served as the competitor in the mobile phase, no obvious change was observed in the retention factor k' of the three ones. Our observations indicated that the binding sites of epimedin B, epimedin C, and icariin on ECD-deleted CaSR are, at least partially, overlapped with cinacalcet instead of NPS2143. This was supported by accumulated evidence that the current positive allosteric ligands, such as cinacalcet, NPS-R568, and calindol, predominantly interact with privileged binding sites located in the 7TMD.[8−10] Therefore, our findings collectively implied that 7TMD-targeted epimedin B, epimedin C, and icariin from the EF extract may be potential allosteric ligands of CaSR. The immobilized ΔCaSR column realized the highly selective discovery of allosteric ligands, since the headless CaSR truncation makes them interact with the 7TMD directly. However, the antiosteoporotic activities of these compounds remain undefined until pharmacological experiments are carried out in the future. The immobilized ΔCaSR column has an advantage of separating binders from nonbinders of the receptor, making it possible for high-throughput screening, as three potential allosteric ligands were screened out from the EF extract. Although the FRET-based assay serves a conformational biosensor to clarify the conformational changes associated with CaSR activation and analyze the allosteric modulation mechanisms during the binding of the ligand alone or the cooperation between two ligands,[39] it is hard to realize high-throughput screening of allosteric ligands. Moreover, FRET signals of fluorophore-labeled CaSR were monitored in the presence of a saturating concentration of calcium (20 mM CaCl₂) and after calcium removal, whereas the chromatographic peaks on the immobilized ΔCaSR column changed when the concentration of CaCl₂ was within the range of 1.5−5.0 mM. In this regard, the immobilized ΔCaSR column has better sensitivity than FRET-based assays.

3.7. Verifying the Allosteric Effect of the Screened Compounds on CaSR Downstream Signaling Events.
CaSR was involved in osteoblastic differentiation and bone mineralization in MC3T3-E1 cells.[40,41] Hence, MC3T3-E1 cells were applied to verify the allosteric effect of the screened compounds from the EF extract in our study. To rule out any direct toxic effects of the tested compounds on cell growth, we measured cell viability using CCK-8 assay kits (Figure 9A). Cell viability (% of control) changed in response to increasing Ca^{2+} concentrations, and the significant improvement was observed in the presence of 4.0 mM Ca^{2+} but the slight reduction was observed at 8.0 mM Ca^{2+}, suggesting that Ca^{2+} did not affect cell viability up to 4.0 mM with 24 h treatment. In agreement with previous observations, the osteoblastic differentiation of MC3T3-E1 cells increased when the cells were exposed to high calcium concentrations (2.8 mM and 3.8 mM).[42] Next, cell viabilities were tested with the other compounds in the presence of 4.0 mM Ca^{2+}, indicating that the optimal concentration for cell growth was 5.0 μM for cinacalcet, 3.2 μM for NPS2143, 5.0 μM for icariin, 2.5 μM for epimedin B, and 2.5 μM for epimedin C. In the following experiments, we used the optimal concentrations of the tested compounds to explore their allosteric effects.

The CaSR binds Ca^{2+} to activate signaling pathways via: $G_{q/11}$-phospholipase C mobilizing intracellular calcium release, and $G_{i/o}$ suppressing cyclic adenosine monophosphate (cAMP).[43] To pinpoint the allosteric effects of the tested compounds on CaSR downstream signaling, we measured intracellular Fluo-4 fluorescence and cAMP levels for different treatments by ELISA kits. The fluorescence intensities displayed in Figure 9B were converted to the calculated Ca^{2+} levels shown in Figure 9C. Compared with the control, slight fluorescence enhancement was observed in the treatment with 4 mM Ca^{2+}, while this Ca^{2+}-induced basal fluorescence intensity was significantly enhanced by 18% with the addition of cinacalcet, but it was significantly quenched by 19% with NPS2143. This is in agreement with a previous study indicating that Ca^{2+} activation of CaSR in medullary thyroid carcinoma cells resulted in Ca^{2+} influx via ion-gated calcium channels in addition to IP3-mediated calcium mobilization,[44] and that cinacalcet and NPS2143 can reinforce agonist-stimulated intracellular Ca^{2+} mobilization.[45] Additionally, the fluorescence enhancement and the elevation of the intracellular Ca^{2+} level were also found in the treatments with icariin, epimedin B, and epimedin C. Especially, epimedin B- and epimedin C-treated groups attained similar maximal fluorescence to the cinacalcet-treated group. The measured intracellular cAMP levels are shown in Figure 9D. In line with the previous observation,[46] herein, the high Ca^{2+} (4 mM) stimulation of the cells led to a significant reduction of 22% of cAMP compared with control cells, and the Ca^{2+}-induced cAMP reduction was further decreased by 18% in the presence of cinacalcet and was conversely increased by 14% in the presence of NPS2143. Taken together, these results demonstrated that CaSR, when modulated by cinacalcet, can elevate the intracellular Ca^{2+} level and inhibit cAMP production in MC3T3-E1 cells, and these observed modulations were completely reversed by NPS2143. Similarly, we found that icariin-, epimedin B-, and epimedin C- treated groups could block the Ca^{2+}-induced cAMP reduction by 10%, 19%, and 22%, respectively, showing comparable effects to cinacalcet and verifying that the screened compounds are potential positive allosteric ligands. Thus, we came to a conclusion that the

immobilized ΔCaSR column will be a promising tool for screening novel allosteric ligands, although the mechanism underlying allosteric ligand-induced receptor bias toward downstream β-arrestin or G-protein signaling remains unclarified in the current work.

4. CONCLUSION

We developed a high-performance affinity chromatographic approach with high selectivity by immobilizing the extracellular domain-deleted CaSR truncation onto silica gels in a site-specific manner as solid-phase materials for column packing to screen allosteric ligands from herbal medicine. The proposed method can circumvent the limitations of cell-based functional assays or radioligand binding assays and simplify the discovery process of allosteric ligands. There are three major advantages: (1) a purified receptor or a reporter fluorophore is not required, thus reducing experimental costs and eliminating purification-inherent drawbacks; (2) measurement of the direct receptor−ligand binding facilitates identification of allosteric ligands targeting uncharacterized binding sites; (3) the method is highly selective, as over 50 compounds in one injection of herbal extract were loaded onto the affinity column, and three potential allosteric ligands were screened out. This approach is specifically suited for the preselection of allosteric ligands since the headless GPCR truncation allows the exposure of the 7TMD to interact directly with allosteric ligands. Although GPCRs differ in TMD accessibility and allosteric site architecture, it has been proven that allosteric modulators can bind to the domain outside the 7TMD of class A GPCRs, the middle of the 7TMD in some GPCRs (FFAR3 class A, CRF1R and PTH1R class B, and mGluR5 class C), and the intracellular surface (outside and inside the 7TMD) of the three different GPCR classes and the orphan GPCRs.[47−49] It is conceivable that the approach can be generalized and extended to other GPCRs, merely requiring the immobilization of a target receptor into the affinity chromatography stationary phase, which advances chromatographic methods in the research field of allosteric ligands.

■ AUTHOR INFORMATION

Corresponding Author

ChaoNi Xiao − *Key Laboratory of Resource Biology and Biotechnology in Western China, Ministry of Education, College of Life Sciences, Northwest University, Xi'an 710069, PR China;* ◉ orcid.org/0000-0002-1372-3414; Phone: +86-29-88302686; Email: xiaochaoni@nwu.edu.cn; Fax: +86-29-88302686

Authors

XianGang Shi − *Key Laboratory of Resource Biology and Biotechnology in Western China, Ministry of Education, College of Life Sciences, Northwest University, Xi'an 710069, PR China*

Ru Xu − *Xi'an International University, Xi'an 710077, PR China*

MeiZhi Jiao − *Key Laboratory of Resource Biology and Biotechnology in Western China, Ministry of Education, College of Life Sciences, Northwest University, Xi'an 710069, PR China*

YaoKun Han − *Key Laboratory of Resource Biology and Biotechnology in Western China, Ministry of Education, College of Life Sciences, Northwest University, Xi'an 710069, PR China*

ShouCheng Zhao − *Key Laboratory of Resource Biology and Biotechnology in Western China, Ministry of Education, College of Life Sciences, Northwest University, Xi'an 710069, PR China*

YiLong Chen − *Key Laboratory of Resource Biology and Biotechnology in Western China, Ministry of Education, College of Life Sciences, Northwest University, Xi'an 710069, PR China*

YiYing Xu − *Key Laboratory of Resource Biology and Biotechnology in Western China, Ministry of Education, College of Life Sciences, Northwest University, Xi'an 710069, PR China*

FengWu Li − *Chemical Drug Department, Xi'an Food and Drug Inspection Institute, Xi'an 710127, PR China*

Complete contact information is available at:
https://pubs.acs.org/10.1021/acsomega.5c01504

■ REFERENCES

(1) Burford, N. T.; Watson, J.; Bertekap, R.; Alt, A. Strategies for the identification of allosteric modulators of G-protein-coupled receptors. *Biochem. Pharmacol.* **2011**, *81* (6), 691−702.

(2) Christopoulos, A.; Kenakin, T. G protein-coupled receptor allosterism and complexing. *Pharmacol. Rev.* **2002**, *54* (2), 323−374.

(3) May, L. T.; Leach, K.; Sexton, P. M.; Christopoulos, A. Allosteric modulation of G protein-coupled receptors. *Annu. Rev. Pharmacol. Toxicol.* **2007**, *47*, 1−51.

(4) Schann, S.; Bouvier, M.; Neuville, P. Technology combination to address GPCR allosteric modulator drug-discovery pitfalls. *Drug Discovery Today: Technol.* **2013**, *10* (2), No. e261−7.

(5) Schann, S.; Mayer, S.; Franchet, C.; Frauli, M.; Steinberg, E.; Thomas, M.; Baron, L.; Neuville, P. Chemical Switch of a Metabotropic Glutamate Receptor 2 Silent Allosteric Modulator into Dual Metabotropic Glutamate Receptor 2/3 Negative/Positive Allosteric Modulators. *J. Med. Chem.* **2010**, *53* (24), 8775−8779.

(6) Muchiri, R. N.; van Breemen, R. B. Drug discovery from natural products using affinity selection-mass spectrometry. *Drug Discovery Today: Technol.* **2021**, *40*, 59−63.

(7) Qin, S. S.; Meng, M. M.; Yang, D. H.; Bai, W. W.; Lu, Y.; Peng, Y.; Song, G. J.; Wu, Y. R.; Zhou, Q. T.; Zhao, S. W.; Huang, X. P.; McCorvy, J. D.; Cai, X. Q.; Dai, A. T.; Roth, B. L.; Hanson, M. A.; Liu, Z. J.; Wang, M. W.; Stevens, R. C.; Shui, W. Q. High-throughput identification of G protein-coupled receptor modulators through affinity mass spectrometry screening. *Chem. Sci.* **2018**, *9* (12), 3192−3199.

(8) Josephs, T. M.; Keller, A. N.; Khajehali, E.; DeBono, A.; Langmead, C. J.; Conigrave, A. D.; Capuano, B.; Kufareva, I.; Gregory, K. J.; Leach, K. Negative allosteric modulators of the human calcium-sensing receptor bind to overlapping and distinct sites within the 7-transmembrane domain. *Br. J. Pharmacol.* **2020**, *177* (8), 1917−1930.

(9) Miedlich, S. U.; Gama, L.; Seuwen, K.; Wolf, R. M.; Breitwieser, G. E. Homology modeling of the transmembrane domain of the human calcium sensing receptor and localization of an allosteric binding site. *J. Biol. Chem.* **2004**, *279* (8), 7254−7263.

(10) Petrel, C.; Kessler, A.; Dauban, P.; Dodd, R. H.; Rognan, D.; Ruat, M. Positive and negative allosteric modulators of the Ca^{2+}-sensing receptor interact within overlapping but not identical binding sites in the transmembrane domain. *J. Biol. Chem.* **2004**, *279* (18), 18990−18997.

(11) Ray, K.; Northup, J. Evidence for distinct cation and calcimimetic compound (NPS 568) recognition domains in the transmembrane regions of the human Ca^{2+} receptor. *J. Biol. Chem.* **2002**, *277* (21), 18908−18913.

(12) Nemeth, E. F.; Fox, J. Calcimimetic Compounds: a Direct Approach to Controlling Plasma Levels of Parathyroid Hormone in Hyperparathyroidism. *Trends Endocrinol. Metab.* **1999**, *10* (2), 66−71.

(13) Nemeth, E. F.; Delmar, E. G.; Heaton, W. L.; Miller, M. A.; Lambert, L. D.; Conklin, R. L.; Gowen, M.; Gleason, J. G.; Bhatnagar, P. K.; Fox, J. Calcilytic compounds: Potent and selective Ca^{2+} receptor antagonists that stimulate secretion of parathyroid hormone. *J. Pharmacol. Exp. Ther.* **2001**, *299* (1), 323−331.

(14) Wu, H.; Lien, E. J.; Lien, L. L.Chemical and pharmacological investigations of Epimedium species: A surveyProgress In Drug ResearchBirkhäuser2003601−57

(15) Chen, X. L.; Li, S. X.; Ge, T.; Zhang, D.-D.; Wang, H. F.; Wang, W.; Li, Y. Z.; Song, X. M. *Epimedium* Linn: A Comprehensive Review of Phytochemistry Pharmacology, Clinical Applications and Quality Control. *Chem. Biodivers.* **2024**, *21*, No. e202400846.

(16) Sun, J.; He, W.; Bai, S. Z.; Peng, X.; Zhang, N.; Li, H. X.; Zhang, W. H.; Wang, L. N.; Shao, X. Q.; He, Y. Q.; Yang, G. D.; Wu, L. Y.; Wang, R.; Xu, C. Q. The expression of calcium-sensing receptor in mouse embryonic stem cells (mESCs) and its influence on differentiation of mESC into cardiomyocytes. *Differentiation* **2013**, *85* (1−2), 32−40.

(17) Sun, Z. G.; Lang, Z. F.; Mu, Y. D.; Li, J.; Xing, C. X.; Yan, L.; Li, S. Therapeutic effect and mechanism of icariin combined with calcium sensitive receptor on mouse gastric cancer cells. *J. Biol. Regul. Homeostatic Agents* **2020**, *34* (5), 1831−1836.

(18) Beigi, F.; Chakir, K.; Xiao, R. P.; Wainer, I. W. G-protein-coupled receptor chromatographic stationary phases. 2. Ligand-induced conformational mobility in an immobilized beta(2)-adrenergic receptor. *Anal. Chem.* **2004**, *76* (24), 7187−7193.

(19) Meng, K. L.; Jiao, M. Z.; Shi, X. G.; Xu, R.; Cheng, P. X.; Lv, H. T.; Zheng, X. H.; Xiao, C. N. A rapid approach to capture the potential bioactive compounds from Rhizoma Drynariae, utilizing disease-associated mutation in calcium sensing receptor to alter the binding affinity for agonists. *J. Pharm. Biomed. Anal.* **2023**, *226*, 115253.

(20) Beigi, F.; Wainer, I. W. Syntheses of immobilized G protein-coupled receptor chromatographic stationary phases: Characterization of immobilized μ and κ opioid receptors. *Anal. Chem.* **2003**, *75* (17), 4480−4485.

(21) Zhao, X.; Li, Q.; Chen, J.; Xiao, C.; Bian, L.; Zheng, J.; Zheng, X.; Li, Z.; Zhang, Y. Exploring drug-protein interactions using the relationship between injection volume and capacity factor. *J. Chromatogr. A* **2014**, *1339*, 137−144.

(22) Jiao, M.; Shi, X.; Han, Y.; Xu, R.; Zhao, S.; Jia, P.; Zheng, X.; Li, X.; Xiao, C. The screened compounds from Ligustri Lucidi Fructus using the immobilized calcium sensing receptor column exhibit osteogenic activity in vitro. *J. Pharm. Biomed. Anal.* **2024**, *245*, 116192.

(23) Stagge, F.; Mitronova, G. Y.; Belov, V. N.; Wurm, C. A.; Jakobs, S. Snap-, CLIP- and Halo-Tag Labelling of Budding Yeast Cells. *PLoS One* **2013**, *8* (10), No. e78745.

(24) Xu, R.; Cheng, P. X.; Meng, K. L.; Li, L. K.; Jiao, M. Z.; Zhao, X.; Jia, P.; Zheng, X. H.; Xiao, C. N. Extracellular domain of human calcium sensing receptor immobilized to silica beads as biomaterial: A rapid chromatographic method for recognizing ligands from complex matrix'Shuangdan'. *J. Chromatogr. B* **2022**, *1208*, 123409.

(25) Cheng, P. X.; Meng, K. L.; Shi, X. G.; Jiao, M. Z.; Han, Y. K.; Li, X.; Liu, P.; Xiao, C. N. Solid-phase extraction with the functionalization of calcium-sensing receptors onto magnetic microspheres as an affinity probe can capture ligands selectively from herbal extract. *Microchim. Acta* **2024**, *191* (1), 34.

(26) Centeno, P. P.; Binmahfouz, L. S.; Alghamdi, K.; Ward, D. T. Inhibition of the calcium-sensing receptor by extracellular phosphate ions and by intracellular phosphorylation. *Front. Physiol.* **2023**, *14*, 1154374.

(27) Ray, K.; Tisdale, J.; Dodd, R. H.; Dauban, P.; Ruat, M.; Northup, J. K. Calindol, a positive allosteric modulator of the human Ca^{2+} receptor, activates an extracellular ligand-binding domain-deleted rhodopsin-like seven-transmembrane structure in the absence of Ca^{2+}. *J. Biol. Chem.* **2005**, *280* (44), 37013−37020.

(28) Wen, T.; Wang, Z.; Chen, X.; Ren, Y.; Lu, X.; Xing, Y.; Lu, J.; Chang, S.; Zhang, X.; Shen, Y.; Yang, X. Structural basis for activation and allosteric modulation of full-length calcium-sensing receptor. *Sci. Adv.* **2021**, *7* (23), No. eabg1483.

(29) Hammerland, L. G.; Krapcho, K. J.; Garrett, J. E.; Alasti, N.; Hung, B. C.; Simin, R. T.; Levinthal, C.; Nemeth, E. F.; Fuller, F. H. Domains determining ligand specificity for Ca2+ receptors. *Mol. Pharmacol.* **1999**, *55* (4), 642−648.

(30) Bertekap, R. L., Jr; Burford, N. T.; Li, Z.; Alt, A. High-Throughput Screening for Allosteric Modulators of GPCRs. *Methods Mol. Biol.* **2015**, *1335*, 223−240.

(31) Geng, Y.; Mosyak, L.; Kurinov, I.; Zuo, H.; Sturchler, E.; Cheng, T. C.; Subramanyam, P.; Brown, A. P.; Brennan, S. C.; Mun, H. C.; et al. Structural mechanism of ligand activation in human calcium-sensing receptor. *Elife* **2016**, *5*, No. e13662.

(32) Zhang, C.; Zhang, T.; Zou, J.; Miller, C. L.; Gorkhali, R.; Yang, J. Y.; Schilmiller, A.; Wang, S.; Huang, K.; Brown, E. M.; et al. Structural basis for regulation of human calcium-sensing receptor by magnesium ions and an unexpected tryptophan derivative co-agonist. *Sci. Adv.* **2016**, *2* (5), No. e1600241.

(33) Leach, K.; Gregory, K. J.; Kufareva, I.; Khajehali, E.; Cook, A. E.; Abagyan, R.; Conigrave, A. D.; Sexton, P. M.; Christopoulos, A. Towards a structural understanding of allosteric drugs at the human calcium-sensing receptor. *Cell Res.* **2016**, *26* (5), 574−592.

(34) Pilepic, K. H.; Yang, Z. L.; Chen, J.; Chen, X. Q.; Wang, Y.; Zhao, J.; Mihaljevic, S.; Li, S. P. Flavonoids in natural and tissue cultured materials of *Epimedium alpinum* identified by using UHPLC-Q-TOF-MS/MS. *Int. J. Mass Spectrom.* **2018**, *434*, 222−232.

(35) Wang, Y. Q.; Guo, Z. M.; Jin, Y.; Zhang, X. L.; Wang, L.; Xue, X. Y.; Liang, X. M. Identification of prenyl flavonoid glycosides and phenolic acids in *Epimedium koreanum* Nakai by Q-TOF-MS combined with selective enrichment on "click oligo (ethylene glycol)" column. *J. Pharm. Biomed. Anal.* **2010**, *51* (3), 606−616.

(36) Zhao, H. Y.; Sun, J. H.; Fan, M. X.; Fan, L.; Zhou, L.; Li, Z.; Han, J.; Wang, B. R.; Guo, D. A. Analysis of phenolic compounds in *Epimedium* plants using liquid chromatography coupled with electrospray ionization mass spectrometry. *J. Chromatogr. A* **2008**, *1190* (1−2), 157−181.

(37) Indran, I. R.; Liang, R. L. Z.; Min, T. E.; Yong, E. L. Preclinical studies and clinical evaluation of compounds from the genus Epimedium for osteoporosis and bone health. *Pharmacol. Ther.* **2016**, *162*, 188−205.

(38) Xu, F. F.; Ding, Y.; Guo, Y. Y.; Liu, B. Y.; Kou, Z. N.; Xiao, W.; Zhu, J. B. Anti-osteoporosis effect of Epimedium via an estrogen-like mechanism based on a system-level approach. *J. Ethnopharmacol.* **2016**, *177*, 148−160.

(39) Liu, H. K.; Yi, P.; Zhao, W. J.; Wu, Y. L.; Acher, F.; Pin, J. P.; Liu, J. F.; Rondard, P. Illuminating the allosteric modulation of the calcium-sensing receptor. *Proc. Natl. Acad. Sci. U. S. A.* **2020**, *117* (35), 21711−21722.

(40) Yamaguchi, T.; Chattopadhyay, N.; Kifor, O.; Butters, R. R., Jr; Sugimoto, T.; Brown, E. M. Mouse osteoblastic cell line (MC3T3-E1) expresses extracellular calcium (Ca2+o)-sensing receptor and its agonists stimulate chemotaxis and proliferation of MC3T3-E1 cells. *J. Bone Miner. Res.* **1998**, *13* (10), 1530−1538.

(41) Ye, C. P.; Yamaguchi, T.; Chattopadhyay, N.; Sanders, J. L.; Vassilev, P. M.; Brown, E. M. Extracellular calcium-sensing-receptor (CaR)-mediated opening of an outward K+ channel in murine MC3T3-E1 osteoblastic cells: Evidence for expression of a functional CaR. *Bone* **2000**, *27* (1), 21−27.

(42) Yamauchi, M.; Yamaguchi, T.; Kaji, H.; Sugimoto, T.; Chihara, K. Involvement of calcium-sensing receptor in osteoblastic differentiation of mouse MC3T3-E1 cells. *Am. J. Physiol.-Endocrinol. Metab.* **2005**, *288* (3), No. E608−E616.

(43) Gorvin, C. M. Calcium-sensing receptor signaling - How human disease informs biology. *Curr. Opin. Endocr. Metab. Res.* **2021**, *16*, 10−28.

(44) Thomsen, A. R. B.; Worm, J.; Jacobsen, S. E.; Stahlhut, M.; Latta, M.; Bräuner-Osborne, H. Strontium Is a Biased Agonist of the Calcium-Sensing Receptor in Rat Medullary Thyroid Carcinoma 6−23 Cells. *J. Pharmacol. Exp. Ther.* **2012**, *343* (3), 638−649.

(45) Leach, K.; Wen, A.; Cook, A. E.; Sexton, P. M.; Conigrave, A. D.; Christopoulos, A. Impact of Clinically Relevant Mutations on the Pharmacoregulation and Signaling Bias of the Calcium-Sensing Receptor by Positive and Negative Allosteric Modulators. *Endocrinology* **2013**, *154* (3), 1105−1116.

(46) Thomsen, A. R. B.; Hvidtfeldt, M.; Bräuner-Osborne, H. Biased agonism of the calcium-sensing receptor. *Cell Calcium* **2012**, *51* (2), 107−116.

(47) Zhang, M.; Lan, X.; Li, X.; Lu, S. Pharmacologically targeting intracellular allosteric sites of GPCRs for drug discovery. *Drug Discovery Today* **2023**, *28* (12), 103803.

(48) Qiao, X.; Li, X.; Zhang, M.; Liu, N.; Wu, Y.; Lu, S.; Chen, T. Targeting cryptic allosteric sites of G protein-coupled receptors as a novel strategy for biased drug discovery. *Pharmacol. Res.* **2025**, *212*, 107574.

(49) Zhang, M.; Chen, T.; Lu, X.; Lan, X.; Chen, Z.; Lu, S. G protein-coupled receptors (GPCRs): advances in structures, mechanisms, and drug discovery. *Signal Transduct. Target. Ther.* **2024**, *9* (1), 88.